AIAA JOURNAL
Vol. 41, No. 7, July 2003

Nonlinear Asymmetric Dynamic Buckling of Isotropic/Laminated Orthotropic Spherical Caps

M. Ganapathi,* S. S. Gupta,† and B. P. Patel‡
Institute of Armament Technology, Pune 411 025, India

Here, the nonlinear dynamic behavior of clamped isotropic/laminated composite spherical caps under suddenly applied loads is studied using a three-noded axisymmetric curved shell element based on field consistency approach. The formulation is based on first-order shear deformation theory, and it includes the in-plane and rotary inertia effects. Geometric nonlinearity is introduced in the formulation using von Karman's strain-displacement relations. The governing equations obtained are solved employing the Newmark's integration technique coupled with a modified Newton–Raphson iteration scheme. The load beyond which the maximum average displacement response shows significant growth in the time history of the shell structure is taken as dynamic buckling pressure. The present model is validated against the available analytical solutions and also with the results evaluated using three-dimensional finite element method. A detailed parametric study is carried out to bring out the effects of shell geometries, orthotropicity, and the number of layers in the cross-ply laminates on the axisymmetric/asymmetric dynamic buckling load of shallow spherical shells.

I. Introduction

THIN spherical shells form an important class of structural components, with many significant applications in engineering fields. These shells subjected to dynamic load could encounter deflections of the order of the thickness of the shell. The dynamic response of such shells can lead to the phenomenon of dynamic snapping or dynamic buckling. Because these kinds of responses cannot be determined accurately using small displacement theory, nonlinear dynamic analysis is required, and such study has received considerable attention in the literature. However, most of the available works are related to axisymmetric behavior of homogeneous, isotropic, or single-layered orthotropic spherical shells subjected to the step pressure load of infinite duration. The present tendency to use fiber-reinforced composite materials for the structural components necessitates the analysis of shells made up of layers of such materials, leading to anisotropic behavior. Moreover, quite often, the asymmetric modes of these shells might be excited as a result of the introduction of slight deviation in perfect axisymmetric loading, geometric imperfection, and/or initial displacement/velocity to the shells. The anisotropic material properties coupled with the asymmetric structural behavior render the failure analysis of these shells quite complex. Hence, there is a growing appreciation of the importance of studying the dynamic response, in particular, dynamic buckling of laminated composite spherical shells and has constituted a major field of research in structural mechanics.

First, a brief review of important contributions to the axisymmetric dynamic snap-through buckling of spherical case is presented here. The analysis of isotropic shallow spherical shells has been carried out by Budiansky and Roth,[1] Simitses,[2] Huang,[3] Stephens and Fulton,[4] Ball and Burt,[5] and Stricklin and Martinez.[6] Budiansky and Roth[1] have employed the Galerkin method, whereas Simitses[2] adopted the Ritz–Galerkin procedure. A finite difference scheme has been introduced in the method of solution by Huang,[3] Stephens and Fulton,[4] and Ball and Burt,[5] whereas Stricklin and Martinez[6] utilized a more efficient finite element procedure. The effect of geometric imperfection on the dynamic buckling load, by employing buckling criterion based on the displacement response, is investigated by Kao and Perrone[7] and Kao[8] based on finite difference method, whereas recently Saigal et al.[9] and Yang and Liaw[10] analyzed using the finite element technique. Lock et al.[11] have carried out experimental study on buckling of shell. The study of axisymmetric dynamic buckling of composite spherical shells has been rather limited and is mainly concerned with the single-layered orthotropic shallow spherical shells using classical lamination theory,[12–15] except the work of Ganapathi and Varadan.[16] Alwar and Sekhar Reddy[12] and Dumir et al.[14] have examined the problem using the method of orthogonal collocation, whereas Chao and Lin[15] have obtained the critical loads based on finite difference scheme including the influence of geometric imperfection. Ganapathi and Varadan[16] have solved the dynamic buckling of laminated composite spherical caps subjected to infinite and finite pulse loading employing shear deformation theory coupled with finite element technique.

Next, for the asymmetric dynamic buckling of isotropic spherical shells, the available studies in the literature that are very few are cited here. Stricklin and Martinez,[6] Stricklin et al.,[17] and Ball and Burt[5] have assumed imperfection in the step load to excite the asymmetric modes and presented results for a shell geometry with few asymmetric modes. Klosner and Longhitano,[18] while obtaining the response of dynamically loaded spherical shells, have considered an asymmetric initial velocity to the shell but numerical results are not presented for the dynamic buckling loads; Akkas[19] has examined the asymmetric dynamic buckling behavior of spherical caps by perturbing few asymmetric modes through the initial displacement and presented very limited results based on the response of asymmetric part of the displacement. It can be inferred that the effect of asymmetric modes of spherical shell with step load of infinite duration on the dynamic buckling characteristics could not be well established with a few available reports in comparison with axisymmetric dynamic buckling case. Furthermore, because of the low transverse shear moduli of advanced composite materials relative to their in-plane moduli transverse shear deformation could be significant even in thin composite structures compared to homogeneous isotropic materials. Hence, it is more appropriate to analyze the dynamics of composite structures including shear deformation and rotary inertia. However, to the authors' knowledge, work on the asymmetric dynamic buckling behavior of laminated composite spherical shells under externally applied pressure seems to be scarce in the literature.

Here, a three-noded shear flexible axisymmetric curved shell element based on semi-analytical approach and the field-consistency principle[20,21] is extended to analyze the axisymmetric/asymmetric

Received 16 May 2002; revision received 20 December 2002; accepted for publication 5 January 2003.

*Professor, Guided Missiles Faculty, Girinagar.
†Scientist, Mechanical Engineering Faculty, Girinagar.
‡Professor, Mechanical Engineering Faculty, Girinagar.

dynamic buckling of laminated composite spherical caps under an externally applied pressure load. Field consistency is a systematic approach to eliminate spurious constraints causing shear and membrane locking when the shear flexible element is applied to thin situation. Geometric nonlinearity is assumed in the present study using von Kármán's strain-displacement relations. In addition, the formulation includes in-plane and rotary inertia effects. The nonlinear governing equations derived are solved employing Newmark numerical integration method in conjunction with the modified Newton–Raphson iteration scheme. For the axisymmetric case the dynamic buckling pressure is taken as the pressure corresponding to a sudden jump in the maximum average displacement in the time history of the shell structure,[1,22] whereas it corresponds to the threshold value of pressure beyond which the asymmetric component of displacement response of shell shows significant growth rate with time.[19,23] Numerical results are presented for isotropic, orthotropic, and laminated cross-ply shallow spherical caps and are compared with the available solutions or those of evaluated based on three-dimensional finite element analysis. A detailed investigation is carried out to bring out the influences of number of layers, geometric parameters, and different asymmetric modes of excitation on the dynamic buckling characteristics of clamped spherical shells.

II. Formulation

An axisymmetric laminated composite shell of revolution is considered with the coordinates s, θ, and z along the meridional, circumferential, and radial/thickness directions, respectively, as shown in Fig. 1. The displacements u, v, w at a point (s, θ, z) from the median surface are expressed as functions of middle-surface displacements u_o, v_o, and w_o, and independent rotations β_s and β_θ of the meridional and hoop sections, respectively, as

$$\begin{aligned} u(s,\theta,z,t) &= u_o(s,\theta,t) + z\beta_s(s,\theta,t) \\ v(s,\theta,z,t) &= v_o(s,\theta,t) + z\beta_\theta(s,\theta,t) \\ w(s,\theta,z,t) &= w_o(s,\theta,t) \end{aligned} \tag{1}$$

where t is the time.

Using the semianalytical approach, u_o, v_o, w_o, β_s, and β_θ are represented by a Fourier series in the circumferential angle θ. For the nth harmonic, following the work of Refs. 24–26, these can be written as

$$\begin{aligned} u_o(s,\theta,t) &= u_o^o(s,t) + \sum_{i=1}^{4}\left[u_o^{c_i}(s,t)\cos(in\theta) + u_o^{s_i}(s,t)\sin(in\theta)\right] \\ v_o(s,\theta,t) &= v_o^o(s,t) + \sum_{i=1}^{4}\left[v_o^{c_i}(s,t)\cos(in\theta) + v_o^{s_i}(s,t)\sin(in\theta)\right] \\ w_o(s,\theta,t) &= w_o^o(s,t) + \sum_{i=1}^{2}\left[w_o^{c_i}(s,t)\cos(in\theta) + w_o^{s_i}(s,t)\sin(in\theta)\right] \\ \beta_s(s,\theta,t) &= \beta_s^o(s,t) + \sum_{i=1}^{2}\left[\beta_s^{c_i}(s,t)\cos(in\theta) + \beta_s^{s_i}(s,t)\sin(in\theta)\right] \\ \beta_\theta(s,\theta,t) &= \beta_\theta^o(s,t) + \sum_{i=1}^{2}\left[\beta_\theta^{c_i}(s,t)\cos(in\theta) + \beta_\theta^{s_i}(s,t)\sin(in\theta)\right] \end{aligned} \tag{2}$$

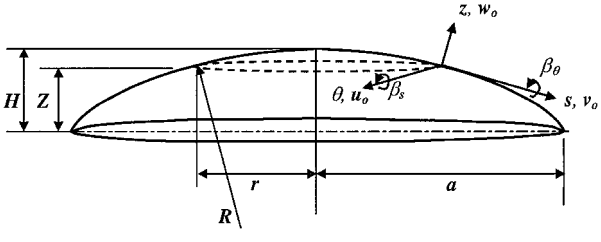

Fig. 1 Geometry and the coordinate system of a spherical cap.

where the superscripts o, c_i, and s_i refer to the amplitudes associated with axisymmetric, cosine, and sine terms.

The preceding displacement variations in the circumferential direction are chosen according to the physics of the large-amplitude asymmetric vibrations of shells of revolution, that is, participation of axisymmetric mode and higher asymmetric modes.[24–26] Additional terms in the in-plane displacements, compared to radial displacement, are added to keep the nonlinear membrane strains consistent.

Using von Kármán's assumption for moderately large deformation, Green's strains can be written in terms of midplane deformations as

$$\{\varepsilon\} = \begin{Bmatrix} \varepsilon_p^L \\ 0 \end{Bmatrix} + \begin{Bmatrix} z\varepsilon_b \\ \varepsilon_s \end{Bmatrix} + \begin{Bmatrix} \varepsilon_p^{NL} \\ 0 \end{Bmatrix} \tag{3}$$

where the membrane strains $\{\varepsilon_p^L\}$, bending strains $\{\varepsilon_b\}$, shear strains $\{\varepsilon_s\}$, and nonlinear in-plane strains $\{\varepsilon_p^{NL}\}$ in Eq. (3) are written as[27]

$$\{\varepsilon_p^L\} = \begin{Bmatrix} \dfrac{\partial u_o}{\partial s} + \dfrac{w_o}{R} \\ \dfrac{u_o \sin\phi}{r} + \dfrac{\partial v_o}{r\partial\theta} + \dfrac{w_o\cos\phi}{r} \\ \dfrac{\partial u_o}{r\partial\theta} - \dfrac{v_o\sin\phi}{r} + \dfrac{\partial v_o}{\partial s} \end{Bmatrix}$$

$$\{\varepsilon_b\} = \begin{Bmatrix} \dfrac{\partial\beta_s}{\partial s} + \dfrac{\partial u_o}{R\partial s} \\ \dfrac{\beta_s\sin\phi}{r} + \dfrac{\partial\beta_\theta}{r\partial\theta} + \dfrac{u_o\sin\phi}{Rr} \\ \dfrac{1}{R}\dfrac{\partial u_o}{r\partial\theta} + \dfrac{\partial v_o}{\partial s}\dfrac{\cos\phi}{r} + \dfrac{\partial\beta_s}{r\partial\theta} + \dfrac{\partial\beta_\theta}{\partial s} - \dfrac{\beta_\theta\sin\phi}{r} \end{Bmatrix}$$

$$\{\varepsilon_s\} = \begin{Bmatrix} \beta_s + \dfrac{\partial w_o}{\partial s} \\ \beta_\theta + \dfrac{\partial w_o}{r\partial\theta} - \dfrac{v_o\cos\phi}{r} \end{Bmatrix}, \qquad \{\varepsilon_p^{NL}\} = \begin{Bmatrix} \dfrac{1}{2}\left(\dfrac{\partial w_o}{\partial s}\right)^2 \\ \dfrac{1}{2}\left(\dfrac{\partial w_o}{r\partial\theta}\right)^2 \\ \dfrac{\partial w_o}{\partial s}\dfrac{\partial w_o}{r\partial\theta} \end{Bmatrix} \tag{4}$$

where r, R, and ϕ are the radius of the parallel circle, radius of the meridional circle, and angle made by the tangent at any point in the shell with the axis of revolution.

If $\{N\}$ represents the stress resultants (N_{ss}, $N_{\theta\theta}$, $N_{s\theta}$) and $\{M\}$ the moment resultants (M_{ss}, $M_{\theta\theta}$, $M_{s\theta}$), one can relate these to membrane strains $\{\varepsilon_p\}(=\{\varepsilon_o^L\}+\{\varepsilon_o^{NL}\})$ and bending strains $\{\varepsilon_b\}$ through the constitutive relations as

$$\begin{Bmatrix} \{N\} \\ \{M\} \end{Bmatrix} = \begin{bmatrix} [A] & [B] \\ [B] & [D] \end{bmatrix} \begin{Bmatrix} \{\varepsilon_p\} \\ \{\varepsilon_b\} \end{Bmatrix} \tag{5}$$

where $[A]$, $[D]$, and $[B]$ are extensional, bending, and bending–extensional coupling stiffness coefficients matrices of the composite laminate. Similarly, the transverse shear force $\{Q\}$ representing the quantities (Q_{sz}, $Q_{\theta z}$,) are related to the transverse shear strains $\{\varepsilon_s\}$ through the constitutive relation as

$$\{Q\} = [E]\{\varepsilon_s\} \tag{6}$$

where $[E]$ is the transverse shear stiffness coefficients matrix of the laminate.

For a composite laminate of thickness h, consisting of N layers with stacking angles ϕ_i $(i = 1, \ldots, N)$ and layer thicknesses $h_i (i = 1, \ldots, N)$, the necessary expressions to compute the stiffness coefficients, available in the literature,[28] are used here.

The potential energy functional $U(\delta)$ is given by

$$U(\boldsymbol{\delta}) = \frac{1}{2}\int_A \big[\{\varepsilon_p\}[\boldsymbol{A}]\{\varepsilon_p\} + \{\varepsilon_p\}[\boldsymbol{B}]\{\varepsilon_b\} + \{\varepsilon_b\}[\boldsymbol{B}]\{\varepsilon_p\} + \{\varepsilon_b\}[\boldsymbol{D}]\{\varepsilon_b\} + \{\varepsilon_s\}[\boldsymbol{E}]\{\varepsilon_s\}\big]\,\mathrm{d}A - \int_A q w_o\,\mathrm{d}A \tag{7}$$

where δ is the vector of degrees of freedom associated to the displacement field in a finite element discretisation and q is the applied external pressure load.

The kinetic energy of the shell is given by

$$T(\boldsymbol{\delta}) = \frac{1}{2}\int_A \big[p\big(\dot{u}_o^2 + \dot{v}_o^2 + \dot{w}_o^2\big) + I\big(\dot{\beta}_s^2 + \dot{\beta}_\theta^2\big)\big]\,\mathrm{d}A \tag{8}$$

where

$$p = \sum_{i=1}^{N}\int_{h_i}^{h_{i+1}} \rho^i\,\mathrm{d}z, \qquad I = \sum_{i=1}^{N}\int_{h_i}^{h_{i+1}} \rho^i z^2\,\mathrm{d}z$$

ρ^i is the mass density of the ith layer, and h_i and h_{i+1} are the z coordinate of the inner and outer surfaces of the ith layer. The dot over the variable denotes the derivative with respect to time.

Following the procedure given in the work of Rajasekaran and Murray,[29] the potential energy functional U given in Eq. (7) is rewritten as

$$U(\delta) = \{\delta\}^T\big[\big(\tfrac{1}{2}\big)[\boldsymbol{K}] + \big(\tfrac{1}{6}\big)[\boldsymbol{N}_1(\delta)] + \big(\tfrac{1}{12}\big)[\boldsymbol{N}_2(\delta)]\big]\{\delta\} + \{\delta\}^T\{\boldsymbol{F}\} \tag{9}$$

where $[\boldsymbol{K}]$ is the linear stiffness matrix, $[\boldsymbol{N}_1]$ and $[\boldsymbol{N}_2]$ are nonlinear stiffness matrices linearly and quadratically dependent on the field variables, respectively, and $\{\boldsymbol{F}\}$ is the load vector. Substituting Eqs. (8) and (9) in Lagrange's equation of motion, the governing equation for the shell are obtained as

$$[\boldsymbol{M}]\{\ddot{\boldsymbol{\delta}}\} + \big[[\boldsymbol{K}] + \tfrac{1}{2}[\boldsymbol{N}_1(\boldsymbol{\delta})] + \tfrac{1}{3}[\boldsymbol{N}_2(\boldsymbol{\delta})]\big]\{\boldsymbol{\delta}\} = \{\boldsymbol{F}\} \tag{10}$$

where $[\boldsymbol{M}]$ is the mass matrix.

Equation (10) is solved using the implicit method, as mentioned by Subbaraj and Dokainish.[30] In this method equilibrium conditions are considered at the same time step for which a solution is sought. If the solution is known at time t and one wishes to obtain the displacements, etc., at time $t + \Delta t$, then the equilibrium equations considered at time $t + \Delta t$ are given as

$$[\boldsymbol{M}]\{\ddot{\boldsymbol{\delta}}\}_{t+\Delta t} + [[\boldsymbol{N}(\delta)]\{\delta\}]_{t+\Delta t} = \{\boldsymbol{F}\}_{t+\Delta t} \tag{11}$$

where $\{\ddot{\boldsymbol{\delta}}\}_{t+\Delta t}$ and $\{\delta\}_{t+\Delta t}$ are the vectors of the nodal accelerations and displacements at time $t + \Delta t$, respectively. $[[\boldsymbol{N}(\delta)]\ \{\delta\}]_{t+\Delta t}$ is the internal force vector at time $t + \Delta t$ and is given as

$$[[\boldsymbol{N}(\delta)]\{\delta\}]_{t+\Delta t} = \Big(\Big[[\boldsymbol{K}] + \big(\tfrac{1}{2}\big)[\boldsymbol{N}_1(\delta)] + \big(\tfrac{1}{3}\big)[\boldsymbol{N}_2(\delta)]\Big]\{\delta\}\Big)_{t+\Delta t} \tag{12}$$

In developing equations for the implicit integration, the internal forces $[\boldsymbol{N}(\delta)]\{\delta\}$ at the time $t + \Delta t$ is written in terms of the internal forces at time t, by using the tangent stiffness approach, as

$$[[\boldsymbol{N}(\delta)]\{\delta\}]_{t+\Delta t} = [[\boldsymbol{N}(\delta)]\{\delta\}]_t + [\boldsymbol{K}_T(\delta)]_t\{\Delta\delta\} \tag{13}$$

where $[\boldsymbol{K}_T(\delta)]_t = [[\boldsymbol{K}] + [\boldsymbol{N}_1] + [\boldsymbol{N}_2]]$ is the tangent stiffness matrix and $\{\Delta\delta\} = \{\delta\}_{t+\Delta t} - \{\delta\}_t$. Substituting Eq. (13) into Eq. (11), one obtains the governing equation at $t + \Delta t$ as

$$[\boldsymbol{M}]\{\ddot{\boldsymbol{\delta}}\}_{t+\Delta t} + [\boldsymbol{K}_T(\delta)]_t\{\Delta\delta\} = \{\boldsymbol{F}\}_{t+\Delta t} - \{[\boldsymbol{N}(\delta)]\{\delta\}\}_t \tag{14}$$

Equation (14), after introducing the Newmark's numerical integration scheme, is rewritten as

$$[\hat{\boldsymbol{K}}]\{\Delta\boldsymbol{\delta}\} = \{\hat{\boldsymbol{F}}\} \tag{15a}$$

where

$$[\hat{\boldsymbol{K}}] = a_o[\boldsymbol{M}] + [\boldsymbol{K}_T(\boldsymbol{\delta})]_t$$

$$\{\hat{\boldsymbol{F}}\} = \{\boldsymbol{F}\}_{t+\Delta t} + [\boldsymbol{M}]\{a_2\{\dot{\boldsymbol{\delta}}\}_t + a_3\{\ddot{\boldsymbol{\delta}}\}_t\} - \{[\boldsymbol{N}(\boldsymbol{\delta})]\{\delta\}\}_t$$

$$a_o = 1/\beta(\Delta t)^2, \qquad a_2 = 1/\beta\Delta t, \qquad a_3 = (1/2\beta) - 1 \tag{15b}$$

Here, the constants α and β are controlling parameters for stability and accuracy of the solution scheme. From the displacement increment $\{\Delta\boldsymbol{\delta}\}$ evaluated from the preceding equation, the displacement and its first and second derivatives (velocity and acceleration) at $t + \Delta t$ can be computed from the following expressions:

$$\{\ddot{\boldsymbol{\delta}}\}_{t+\Delta t} = a_o\{\Delta\boldsymbol{\delta}\} - a_2\{\dot{\boldsymbol{\delta}}\}_t - a_3\{\ddot{\boldsymbol{\delta}}\}_t$$

$$\{\dot{\boldsymbol{\delta}}\}_{t+\Delta t} = a_1\{\Delta\boldsymbol{\delta}\} - a_4\{\dot{\boldsymbol{\delta}}\}_t - a_5\{\ddot{\boldsymbol{\delta}}\}_t$$

$$\{\boldsymbol{\delta}\}_{t+\Delta t} = \{\boldsymbol{\delta}\}_t + \{\Delta\boldsymbol{\delta}\} \tag{16}$$

where $a_1 = \alpha/\beta\Delta t$, $a_4 = (\alpha/\beta) - 1$, and $a_5 = (\Delta t/2)\,(\alpha/\beta - 1)$.

To improve the solution accuracy and to avoid numerical instabilities, it is necessary to employ iteration within each time, thus maintaining the equilibrium. The equilibrium is achieved for each time step through modified Newton–Raphson iteration until the convergence criteria suggested by Bergan and Clough[31] are satisfied within the specific tolerance limit of less than 1%.

III. Dynamic Buckling Criteria

Criteria for the static buckling of axisymmetric shallow spherical shell are well defined, whereas this is not so for the dynamic case. It requires the evaluation of the transient response of the shell for different load amplitudes. However, the dynamic buckling criterion suggested by Budiansky and Roth[1] is generally accepted because the results obtained by various investigators by different numerical techniques using the criterion are in reasonable agreement with each other. This criterion is based on the plots of the peak nondimensional average displacement in the time history of the structure with respect to the amplitude of the pressure load (e.g., see Fig. 2). The average displacement Δ is defined as

$$\Delta = \frac{\int_0^a r w_o\,\mathrm{d}r}{\int_0^a r Z\,\mathrm{d}r} \tag{17}$$

The numerator is the volume generated by the shell deformation, and the denominator corresponds to the original volume under the spherical cap. Z is the height of a point on the middle surface of

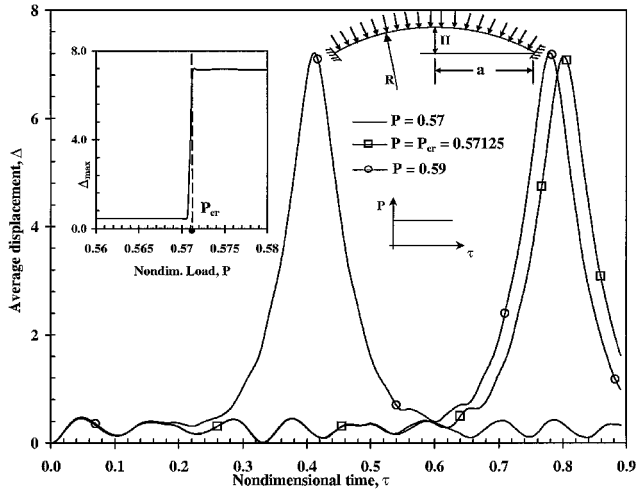

Fig. 2 Average displacement vs nondimensional time for isotropic spherical cap ($\lambda = 7$, axisymmetric case).

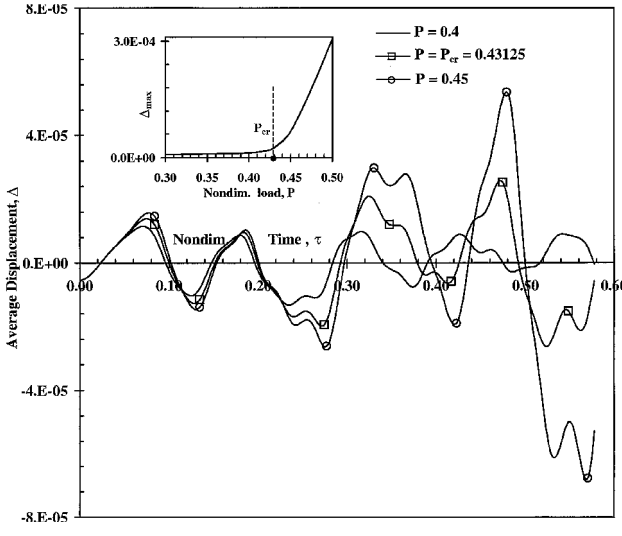

Fig. 3 Average displacement vs nondimensional time for isotropic spherical cap ($\lambda = 7$, asymmetric case with $n = 3$).

the shell. There is a load range where a sharp jump in peak average displacement occurs for a small change in load magnitude. The inflection point of the load-deflection curve is considered as the dynamic buckling load.

For asymmetric dynamic buckling analysis of spherical shells, there is no well-understood and generally accepted criterion available so far. Furthermore, the available numerical results to obtain a reasonable conclusion on the criterion are very few, compared to the axisymmetric case. The criterion adopted by Fulton and Barton[22] and Akkas[19] is somewhat similar to that of the axisymmetric case. It is based on the plots of the peak nondimensional average asymmetric component of the displacement in the time history of the structure against the amplitude of the pressure load. However, as there is no occurrence of a sudden jump in peak average displacement associated with asymmetric part of the deformation over a load range, the load corresponding to the inflection point on the load-deflection curve beyond which the asymmetric part of the displacement response reveals significant growth rate is considered as dynamic buckling load (e.g., see Fig. 3).

IV. Element Description

The element employed here is a three-noded C^o continuous shear flexible axisymmetric element with 33 degrees of freedom $(u_o^o, u_o^{c1}, u_o^{s1}, u_o^{c2}, u_o^{s2}, u_o^{c3}, u_o^{s3}, u_o^{c4}, u_o^{s4}, v_o^o, v_o^{c1}, v_o^{s1}, v_o^{c2}, v_o^{s2}, v_o^{c3}, v_o^{s3}, v_o^{c4}, v_o^{s4}, w_o^o, w_o^{c1}, w_o^{s1}, w_o^{c2}, w_o^{s2}, \beta_s^o, \beta_s^{c1}, \beta_s^{s1}, \beta_s^{c2}, \beta_s^{s2}, \beta_\theta^o, \beta_\theta^{c1}, \beta_\theta^{s1}, \beta_\theta^{c2}, \beta_\theta^{s2})$ per node, that is, from Eq. (2). The field variables are expressed in terms of their nodal values using shape functions as

$$\left(u_o^o, u_o^{c1}, u_o^{s1}, \ldots, \beta_\theta^{s1}, \beta_\theta^{c2}, \beta_\theta^{s2}\right) = \sum_{i=1}^{3} \bar{N}_i^0 \left(u_{oi}^o, u_{oi}^{c1}, u_{oi}^{s1}, \ldots, \beta_{\theta i}^{s1}, \beta_{\theta i}^{c2}, \beta_{\theta i}^{s2}\right) \tag{18}$$

where $\bar{N}_1^0 = (\xi^2 - \xi)/2$, $\bar{N}_2^0 = (1 - \xi^2)$, $\bar{N}_3^0 = (\xi^2 + \xi)/2$; ξ is the local meridional coordinate of the element. Here, $\bar{N}_i^0$ are the original shape functions.

If the interpolation functions for three-noded element are used directly to interpolate the 33 field variables $(u_o^o, u_o^{c1}, u_o^{s1}, \ldots, \beta_\theta^{s1}, \beta_\theta^{c2}, \beta_\theta^{s2})$ in deriving the transverse shear and membrane strains, the element will lock and show oscillations in the shear and membrane stresses. Field consistency requires that the membrane and transverse shear strains must be interpolated in a consistent manner. Thus, while substituting the variable β_s [defined in Eq. (2)] in the expression for $\{\varepsilon_s\}$ given in Eq. (4) the terms $\beta_s^o, \beta_s^{c1}, \beta_s^{s1}, \beta_s^{c2}, \beta_s^{s2}$ have to be consistent with field functions $\partial w_o^o/\partial s, \partial w_o^{c1}/\partial s, \partial w_o^{s1}/\partial s, \partial w_o^{c2}/\partial s, \partial w_o^{s2}/\partial s$, respectively, as shown in the works of Balakrishna and Sarma,[20] Ganapathi et al.,[21] and Prathap and Ramesh Babu.[32] Similarly, while substituting the variables w_o and (u_o and v_o) in Eq. (4) for membrane strain $\{\varepsilon_p^L\}$ expressions, the terms $(w_o^o, w_o^{c1}, w_o^{s1}, w_o^{c2}, w_o^{s2})$ and $[(u_o^o, u_o^{c1}, u_o^{s1}, \ldots, u_o^{c4}, u_o^{s4})$ and $(v_o^o, v_o^{c1}, v_o^{s1}, \ldots, v_o^{c4}, v_o^{s4})]$ have to be consistent with the field functions $(\partial u_o^o/\partial s, \partial u_o^{c1}/\partial s, \partial u_o^{s1}/\partial s, \ldots, \partial u_o^{c4}/\partial s, \partial u_o^{s4}/\partial s)$ and $(\partial v_o^o/\partial s, \partial v_o^{c1}/\partial s, \partial v_o^{s1}/\partial s, \ldots, \partial v_o^{c4}/\partial s, \partial v_o^{c4}/\partial s)$, respectively, depending on the strain components. This is achieved by using the field redistributed substitute shape functions to interpolate those specific terms that must be consistent as described by Prathap and Ramesh Babu.[32] The substitute interpolation functions obtained using method of least squares are given as

$$\bar{N}_1^1 = \left(\tfrac{1}{3} - \xi\right)/2, \qquad \bar{N}_2^1 = \tfrac{2}{3}, \qquad \bar{N}_3^1 = \left(\tfrac{1}{3} + \xi\right)/2 \tag{19}$$

where $\bar{N}_1^1$, $\bar{N}_2^1$, and $\bar{N}_3^1$ are consistent with $\bar{N}_{1,\xi}^0$, $\bar{N}_{2,\xi}^0$, and $\bar{N}_{3,\xi}^0$, respectively.

The element derived in this fashion behaves very well for both thick and thin situations and permits the greater flexibility in the choice of integration order for the energy terms. It has good convergence and has no spurious rigid modes.

V. Results and Discussion

The study here has been concerned with axisymmetric/asymmetric dynamic buckling behavior of clamped isotropic/laminated composite spherical caps. Because the finite element used here is based on the field consistency approach, an exact integration is employed to evaluate all of the strain-energy terms. The shear correction factor, which is required in a first-order theory to account for the variation of transverse shear stresses, is taken as $\frac{5}{6}$. For the present analysis, based on progressive mesh refinement, 15-element idealization is found to be adequate in modeling the spherical caps. The initial conditions for the nonlinear axisymmetric dynamic case are assumed as zero values for the displacements and velocities, whereas for the asymmetric dynamic response analysis nonzero values for displacements and zero values for the velocities are considered. The initial nonzero displacement vectors are assumed to be proportional to the normalized linear flexural asymmetric mode vectors and then scaled up by multiplying the mode vectors with a very small value for the perturbation of asymmetric mode of the spherical shell. From the dynamic response curves the load amplitudes and the corresponding maximum average displacements are obtained for applying the buckling criteria. The constants α and β in Newmark's method are taken as 0.5 and 0.25, which correspond to the unconditionally stable scheme in linear analysis. Because there is no estimate of the time step for the nonlinear dynamic analysis available in the literature, the critical time step of conditionally stable finite difference schemes[33,34] is introduced as a guide, and a convergence study was conducted to select a time step that yields a stable and accurate solution.

The material properties assumed in the present analysis are as follows.

Isotropic case:

$$E = 210\ \text{GPa}, \qquad \nu = 0.3, \qquad \rho = 7800\ \text{kg/m}^3$$

Orthotropic case:

$$E_L/E_T = 25.0, \qquad G_{LT}/E_T = 0.5, \qquad G_{TT}/E_T = 0.2$$

$$\nu_{LT} = 0.25, \qquad E_T = 1\ \text{GPa}, \qquad \rho = 1500\ \text{kg/m}^3$$

where E, G, and ν are Young's modulus, shear modulus, and Poisson's ratio. Subscripts L and T are the longitudinal and transverse directions respectively with respect to the fibers. All of the layers are of equal thickness. The ply angles are measured with respect to the meridional axis.

The clamped boundary conditions at the base of the cap are taken as

$$u_o^o = u_o^{c1} = u_o^{s1} = u_o^{c2} = u_o^{s2} = u_o^{c3} = u_o^{s3} = u_o^{c4} = u_o^{s4} = v_o^o$$
$$= v_o^{c1} = v_o^{s1} = v_o^{c2} = v_o^{s2} = v_o^{c3} = v_o^{s3} = v_o^{c4} = v_o^{s4} = 0$$
$$w_o^o = w_o^{c1} = w_o^{s1} = w_o^{c2} = w_o^{s2} = \beta_s^o = \beta_s^{c1} = \beta_s^{s1} = \beta_s^{c2}$$
$$= \beta_s^{s2} = \beta_\theta^o = \beta_\theta^{c1} = \beta_\theta^{s1} = \beta_\theta^{c2} = \beta_\theta^{s2} = 0 \quad (20)$$

The results of nondimensional dynamic pressure P_{cr} are presented for isotropic, orthotropic, and cross-ply laminates for different values of the geometrical parameter λ. P_{cr} and λ are given by

$$P_{cr} = \tfrac{1}{8}[3(1-\nu^2)]^{\frac{1}{2}}(h/H)^2(qa^4/Eh^4) \quad (21)$$

$$\lambda = 2[3(1-\nu^2)]^{\frac{1}{4}}(H/h)^{\frac{1}{2}} \quad (22)$$

Here, H and a are the central shell rise and base radius, respectively. E and ν correspond to the isotropic case. For the chosen shell parameter and lamination scheme the dynamic buckling study is conducted for step loading of infinite duration. The length of response calculation time $\tau\{=\sqrt{(Eh^2/[12(1-\nu^2)\rho a^4])}t\}$ in the present study is varied between one and two with the criterion that in the neighborhood of the buckling τ is large enough to allow deflection–time curves to fully develop. The time step selected, based on the convergence study, is $\delta\tau = 0.002$. The value selected for τ and $\delta\tau$ is of the same order as that of Ball and Burt,[5] Chao and Lin,[15] and Kao and Perrone.[7]

Before proceeding for the detailed study of the nonlinear asymmetric dynamic buckling characteristics, the formulation developed herein is validated against the axisymmetric buckling of isotropic spherical shells subjected to uniform external pressure of infinite duration. The nonlinear axisymmetric dynamic response history with time for the geometric shell parameter $\lambda = 7$ is shown in Fig. 2 for different externally applied pressures. Further, using such plots, the variation of maximum average displacement with applied load obtained for $\lambda = 7$ is also highlighted in Fig. 2 for predicting the critical load. The critical dynamic pressures calculated for various geometrical parameter values are presented in Fig. 4 along with those of available analytical/numerical results,[3,4,12,16] and they are, in general, found to be in good agreement.

Next, for the isotropic spherical caps, considering different values for the geometrical parameter λ, the dynamic buckling loads are evaluated based on asymmetric nonlinear dynamic response of shells subjected to externally applied pressure. This study is carried out perturbing the different asymmetric modes (circumferential wave number n). Figure 3 exhibits the dynamic response pattern of average asymmetric displacement component of shell ($\lambda = 7$) with time and, in turn, the variation of maximum average displacement with applied loads. The influence of various asymmetric modes on the critical dynamic load is also investigated and depicted in Fig. 5. It is revealed from Fig. 5 that the results available in the literature[5,19] are in fairly good agreement with the present solutions, and the buckling criterion used in the present study is based on the growth rate of asymmetric mode response with time. However, for the $\lambda = 7.5$ case the present model predicts a higher value for the critical load than those of Akkas[19] and is more than those of the axisymmetric case. Furthermore, it can be seen from Fig. 5 that this particular shell appears to be buckled in axisymmetric mode rather than in asymmetric deformation as pointed out in the work of Stricklin and Martinez[6] while examining the asymmetric mode of buckling. The predicted axisymmetric critical load is in fairly good agreement with the available experimental result.[11] It is further noticed from Fig. 5 that the values of critical load corresponding to $\lambda = 6$ and 12 obtained by Ball and Burt[5] match very well with those of present results pertaining to asymmetric mode $n = 3$. However, the mode numbers reported in Ref. 5 for the shell parameter $\lambda = 6$ and 12 are $n = 2$ and 5 or 6, respectively. It can also be observed from this figure that the present result corresponding to $n = 5$ is somewhat close to that of Ref. 5. The asymmetric mode is initiated through the asymmetric load in Ref. 5, whereas in the present study it is introduced considering asymmetric type of initial displacement. It can be observed

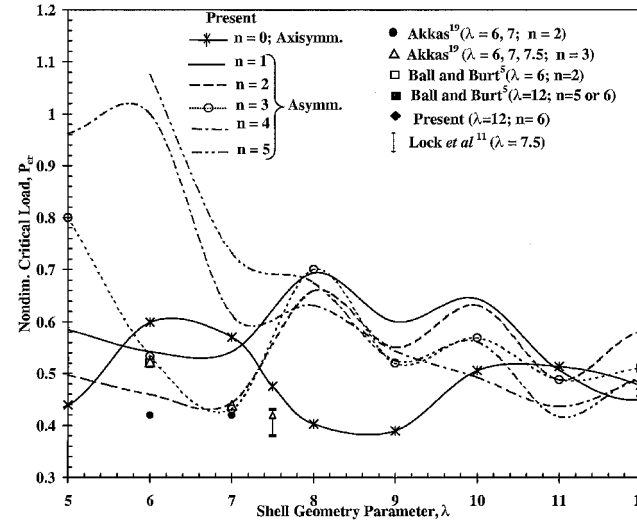

Fig. 5 Nondimensional critical load (for axisymmetric and asymmetric cases) vs shell geometry parameter for isotropic spherical cap.

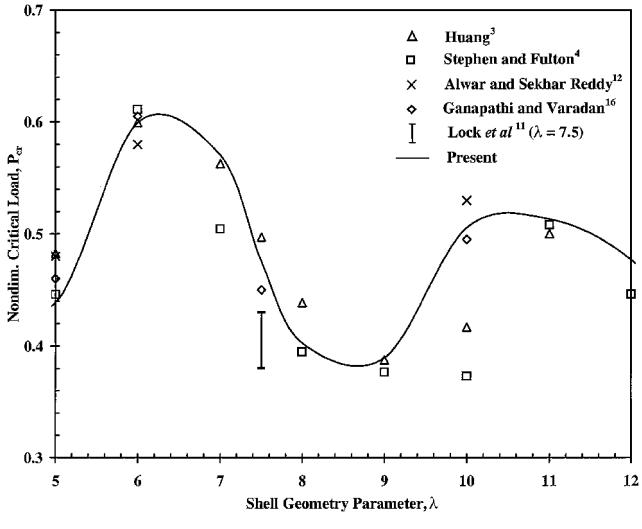

Fig. 4 Comparison of axisymmetric nondimensional critical load for isotropic spherical cap.

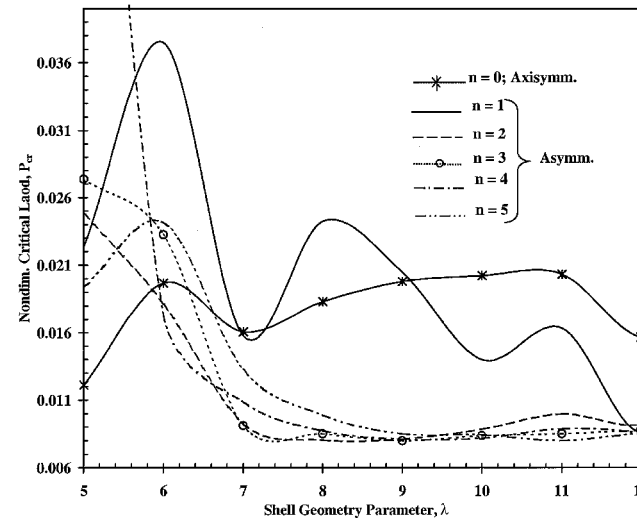

Fig. 6 Nondimensional critical load (for axisymmetric and asymmetric cases) vs shell geometry parameter for single-layer orthotropic spherical cap.

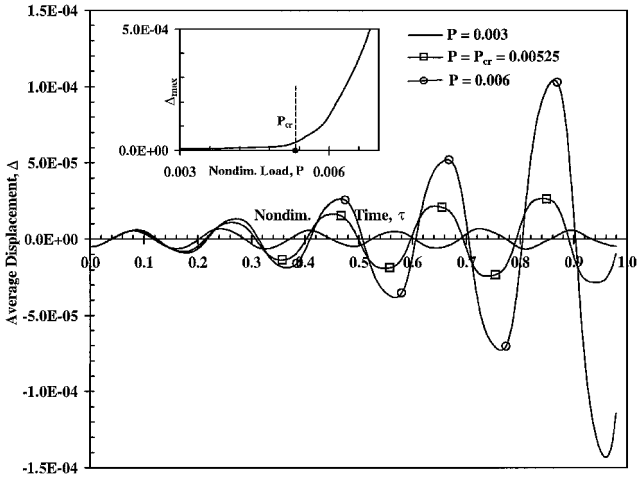

Fig. 7 Average displacement vs nondimensional time for two-layered cross-ply (0/90 deg) spherical cap ($\lambda = 7$, asymmetric case with $n = 3$).

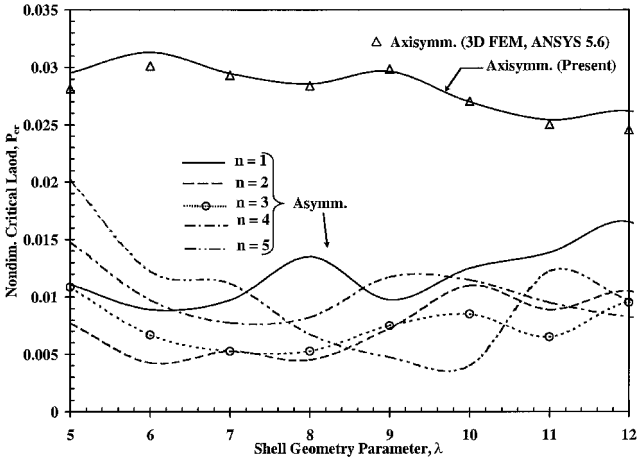

Fig. 8 Nondimensional critical load (for axisymmetric and asymmetric cases) vs shell geometry parameter for two-layered cross-ply (0/90 deg) spherical cap.

from Fig. 5 that the axisymmetric type of dynamic buckling occurs for very shallow shells and also for shell parameters in the transition region between moderately shallow and deep cases. The asymmetric buckling deformation, in general, dominates the moderately shallow shells under lower asymmetric modes and deep shell regions under higher modes. It can be further inferred that, among the asymmetric cases, the difference in the predicted critical loads is high for the shell geometrical parameter in the shallow region, and it reduces with the increase in the value of shell parameter. It, however, largely depends on the perturbation of asymmetric vibration mode.

The investigation for dynamic buckling analysis of single-layer orthotropic shells is carried out, and the results are presented in Fig. 6. Unlike the isotropic case, it can be observed that, except for very shallow cases, the asymmetric mode is important in predicting the critical loads over a fairly wider range of shell parameters considered here. For the higher values of geometrical parameter, the difference in the critical loads calculated using different asymmetric modes is less. The predicted asymmetric critical load is, in general, less than those of axisymmetric cases for a wider range of geometrical parameter, and the load magnitudes are also low compared to those of isotropic case.

Similar study is made for the laminated cross-ply spherical shells. The dynamic response evaluated as a result of different load levels for $\lambda = 7$ is shown in Fig. 7. From such a plot the relationship between the maximum average displacement and applied pressure load obtained is also depicted in Fig. 7. It is seen that there is significant growth rate in the value of the average displacement when the external pressure reaches the value $P_{cr} = 0.00525$ for the two-

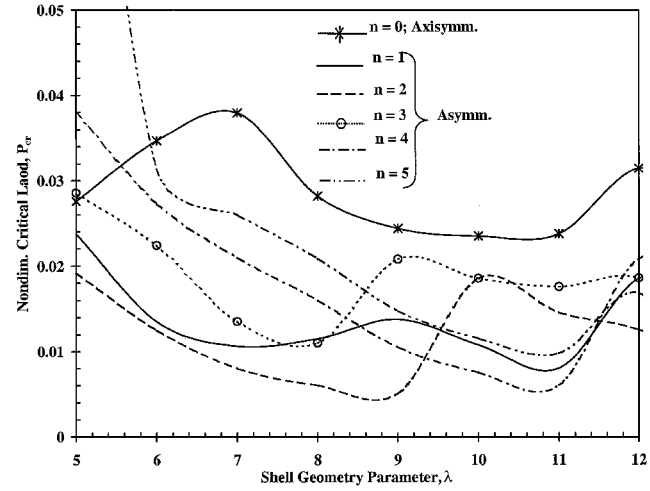

Fig. 9 Nondimensional critical load (for axisymmetric and asymmetric cases) vs shell geometry parameter for eight-layered cross-ply $(0/90\ \text{deg})_4$ spherical cap.

layered cross-ply spherical cap. The dynamic buckling values obtained in this manner are brought out in Figs. 8 and 9 for two- and eight-layered cross-ply spherical caps. The efficacy of the present formulation is tested considering two-layered laminated shells, and the results are in very good agreement with the three-dimensional finite element solution for the axisymmetric dynamic buckling case (Fig. 8). It is revealed from Figs. 8 and 9 that the axisymmetric dynamic buckling load, in general, is very high compared to that of the asymmetric buckling case. Because of bending–stretching coupling, the predicted asymmetric dynamic critical loads for the two-layered case are less compared to those of the single-layer orthotropic shell. The influence of the asymmetric mode on the eight-layered cross-ply case is qualitatively similar to those of two-layered shell, but the critical loads evaluated are higher than those of the two-layered case for the chosen circumferential mode, as expected. It also brings out that the variation in the buckling loads obtained based on axisymmetric and asymmetric modes is less with the increase in number of layers. Furthermore, the buckling trend of laminated shells in asymmetric mode, especially a multilayered one, is somewhat close to the behavior of isotropic case. In general, it can be opined that the lowest critical dynamic buckling load of a given spherical cap significantly depends on its geometrical parameter value, number of layers, and type of mode of excitation.

VI. Conclusions

Asymmetric dynamic buckling of clamped spherical caps, made up of isotropic, orthotropic, and laminated composite materials, subjected to externally applied pressure, has been investigated through transient dynamic response analysis. A three-noded axisymmetric curved shell element based on the field consistency principle has been employed for this purpose. Numerical results obtained here for an isotropic case are found to be in fairly good agreement with the previous findings and also with the solutions obtained using a three-dimensional finite element model. From the detailed study the following observations can be made:

1) For moderately shallow isotropic spherical caps the lowest critical pressure, in general, corresponds to asymmetric deformation of shells with lower circumferential wave numbers, whereas it is at higher asymmetric modes for deep shell cases.

2) For the orthotropic case the asymmetric modes produce the least loads over a wider range of shell parameter compared to the isotropic case.

3) The influence of asymmetric mode on the dynamic buckling load is significant for very shallow shells, but the axisymmetric buckling mode yields the lowest critical values.

4) The difference in the buckling values predicted among various asymmetric modes decreases rapidly with an increase in the value of the shell parameter.

5) The bending–stretching coupling as a result of layup, in general, reduces the buckling loads, and the asymmetric buckling dominates the failure of various shell geometric parameters considered here.

6) With the increase in the number of layers, the buckling behavior is qualitatively similar to those of isotropic case.

7) For a given spherical cap the critical dynamic buckling load, in general, depends on initial condition, geometrical parameter, and layup.

References

[1]Budiansky, B., and Roth, R. S., "Axisymmetric Dynamic Buckling of Clamped Shallow Spherical Shells," NASA TND-1510, Dec. 1962, pp. 597–606.

[2]Simitses, G. J., "Axisymmetric Dynamic Snap-Through Buckling of Shallow Spherical Caps," *AIAA Journal*, Vol. 5, 1967, pp. 1019–1021.

[3]Huang, N. C., "Axisymmetric Dynamic Snap-Through of Elastic Clamped Shallow Shell," *AIAA Journal*, Vol. 7, 1969, pp. 215–220.

[4]Stephens, W. B., and Fulton, R. E., "Axisymmetric Static and Dynamic Buckling of Spherical Caps due to Centrally Distributed Pressure," *AIAA Journal*, Vol. 7, 1969, pp. 2120–2126.

[5]Ball, R. E., and Burt, J. A., "Dynamic Buckling of Shallow Spherical Shells," *Journal of Applied Mechanics*, Vol. 41, 1973, pp. 411–416.

[6]Stricklin, J. A., and Martinez, J. E., "Dynamic Buckling of Clamped Spherical Cap Under Step Pressure Loadings," *AIAA Journal*, Vol. 7, 1969, pp. 1212, 1213.

[7]Kao, R., and Perrone, N., "Dynamic Buckling of Axisymmetic Spherical Caps with Initial Imperfection," *Computers and Structures*, Vol. 9, 1978, pp. 463–473.

[8]Kao, R., "Nonlinear Dynamic Buckling of Spherical Caps with Initial Imperfection," *Computers and Structures*, Vol. 12, 1980, pp. 49–63.

[9]Saigal, S., Yang, T. Y., and Kapania, R. K., "Dynamic Buckling of Imperfection Sensitive Shell Structures," *Journal of Aircraft*, Vol. 24, 1987, pp. 718–724.

[10]Yang, T. Y., and Liaw, D. G., "Elastic-Plastic Dynamic Buckling of Thin Shell Finite Elements with Asymmetric Imperfections," *AIAA Journal*, Vol. 25, 1988, pp. 479–485.

[11]Lock, M. H., Okubo, S., and Whitter, J. S., "Experiments on the Snapping of a Shallow Dome Under a Step Pressure Load," *AIAA Journal*, Vol. 6, 1968, pp. 1320–1326.

[12]Alwar, R. S., and Sekhar Reddy, B., "Dynamic Buckling of Isotropic and Orthotropic Shallow Spherical Caps with Circular Hole," *International Journal of Mechanical Sciences*, Vol. 21, 1979, pp. 681–688.

[13]Ganapathi, M., and Varadan, T. K., "Dynamic Buckling of Orthotropic Shallow Spherical Shells," *Computers and Structures*, Vol. 15, 1982, pp. 517–520.

[14]Dumir, P. C., Gandhi, M. L., and Nath, Y., "Axisymmetric Static and Dynamic Buckling of Orthotropic Shallow Spherical Caps with Flexible Supports," *Acta Mechanica*, Vol. 52, 1984, pp. 93–106.

[15]Chao, C. C., and Lin, I. S., "Static and Dynamic Snap-Through of Orthotropic Spherical Caps," *Composite Structures*, Vol. 14, 1990, pp. 281–301.

[16]Ganapathi, M., and Varadan, T. K., "Dynamic Buckling of Laminated Anisotropic Spherical Caps," *Journal of Applied Mechanics*, Vol. 62, 1995, pp. 13–19.

[17]Stricklin, J. A., and Martinez, J. E., Tillerson, J. R., Hong, J. H., and Haisler, W. E., "Nonlinear Dynamic Analysis of Shells of Revolution by Matrix Displacement Method," *AIAA Journal*, Vol. 9, 1971, pp. 629–636.

[18]Klosner, J. M., and Longhitano, R., "Nonlinear Dynamics of Hemispherical Shells," *AIAA Journal*, Vol. 11, 1973, pp. 1117–1122.

[19]Akkas, N., "Bifurcation and Snap-Through Phenomena in Asymmetric Dynamic Analysis of Shallow Spherical Shells," *Computers and Structures*, Vol. 6, 1976, pp. 241–251.

[20]Balakrishna, C., and Sarma, B. S., "Analysis of Axisymmetric Shells Subjected to Asymmetric Loads Using Field Consistent Shear Flexible Curved Element," *Journal of the Aeronautical Society of India*, Vol. 41, 1989, pp. 89–95.

[21]Ganapathi, M., Varadan, T. K., and Jijen, J., "Field-Consistent Element Applied to Flutter Analysis of Circular Cylindrical Shells," *Journal of Sound and Vibration*, Vol. 171, 1994, pp. 509–527.

[22]Fulton, R. E., and Barton, F. W., "Dynamic Buckling of Shallow Arches," *Journal of Engineering Mechanics Division*, Vol. EM2, 1971, pp. 865–877.

[23]Simitses, G. J., *Dynamic Stability of Suddenly Loaded Structures*, Springer-Verlag, New York, 1989.

[24]Ueda, T., "Nonlinear Free Vibrations of Conical Shells," *Journal of Sound and Vibration*, Vol. 64, 1979, pp. 85–95.

[25]Tong, P., and Pian, T. H. H., "Postbuckling Analysis of Shells of Revolution by the Finite Element Method," *Thin Shell Structures*, edited by Y. C. Fung and E. E. Sechler, Prentice–Hall, Upper Saddle River, NJ, 1974, pp. 435–452.

[26]Amabili, M., Pellicano, F., and Paidoussis, M. P., "Non-Linear Dynamics and Stability of Circular Cylindrical Shells Containing Flowing Fluid, Part II: Large Amplitude Vibrations Without Flow," *Journal of Sound and Vibration*, Vol. 228, 1999, pp. 1103–1124.

[27]Kraus, H., *Thin Elastic Shells*, Wiley, New York, 1967.

[28]Jones, R. M., *Mechanics of Composite Materials*, McGraw–Hill, New York, 1975.

[29]Rajasekaran, S., and Murray, D. W., "Incremental Finite Element Matrices," *Journal of the Structural Division*, Vol. 99, 1973, pp. 2423–2438.

[30]Subbaraj, K., and Dokainish, M. A., "A Survey of Direct Time-Integration Methods in Computational Structural Dynamics II: Implicit Methods," *Computers and Structures*, Vol. 32, 1989, pp. 1387–1401.

[31]Bergan, P. G., and Clough, R. W., "Convergence Criteria for Iterative Process," *AIAA Journal*, Vol. 10, 1972, pp. 1107, 1108.

[32]Prathap, G., and Ramesh Babu, C., "A Field-Consistent Three-Noded Quadratic Curved Axisymmetric Shell Element," *International Journal for Numerical Methods in Engineering*, Vol. 23, 1986, pp. 711–723.

[33]Leech, J. N., "Stability of Finite Difference Equations for the Transient Response of a Flat Plate," *AIAA Journal*, Vol. 3, 1965, pp. 1772, 1773.

[34]Tsui, T. Y., and Tong, P., "Stability of Transient Solution of Moderately Thick Plate by Finite Difference Method," *AIAA Journal*, Vol. 9, 1971, pp. 2062, 2063.

S. Saigal
Associate Editor